

Traceable mmWave Modulated-Signal Measurements for OTA Test

Joshua M. Kast^{1,2}, Paritosh Manurkar^{1,3}, Kate A. Remley¹, Rob Horansky¹, Dylan F. Williams¹

¹National Institute of Standards and Technology, Boulder, CO, USA,

²Colorado School of Mines, Golden, CO, USA, ³University of Colorado, Boulder, CO, USA

Abstract — We present a single-instrument solution to traceable mmWave wide-band modulated-signal measurement in OTA test environments. The approach can be used to characterize transmitters, receivers and transceivers using either time-domain or frequency-domain multiplexing on a fine frequency grid.

Index Terms — Calibration, measurement, modulated signal, over-the-air test, large-signal vector network analyzer.

I. INTRODUCTION

We integrate a large-signal network analyzer (LSNA) with an over-the-air (OTA) test environment and external phase reference to allow for the traceable measurement of repetitive wideband millimeter-wave (mmWave) modulated signals on arbitrary frequency grids. The LSNA measurements are used to characterize the modulated signals in the OTA environment, characterize the forward and backward waves within the transmission lines, and mismatch-correct the measurement results.

We calibrate the LSNA on an arbitrary frequency grid by extending the electrical cross-frequency phase calibration of [1] to mmWave frequency bands. The approach is ideal for efficiently predistorting and measuring long repetitive modulated signals and simultaneously capturing intermodulation and other mixing products created by non-linear processes at intermediate (IF), local-oscillator (LO) and radio-frequency (RF) signals on arbitrary and/or finely spaced frequency grids on each forward and backward channel in the system. Our approach also enables LSNA-based OTA test for linearization [2] at mmWave frequencies on arbitrary grids and a complete uncertainty analysis using the NIST Microwave Uncertainty Framework (MUF) [3].

Finally, our approach considerably extends our prior work [4], where we demonstrated the measurement of the linear response of up-converting and down-converting receivers and transmitters in an OTA environment, but not measurements of intermodulation products or measurements on an arbitrary grid. In contrast with the 28 GHz measurements of [5], we use a sampling oscilloscope to enable traceable phase calibration of the LSNA at each individual measurement frequency.

II. OTA TEST SYSTEM

Fig. 1 shows photographs of NIST's Synthetic Aperture Measurement Uncertainty for Angle of Incidence (SAMURAI)

measurement system in a custom-built OTA test environment. The SAMURAI system uses a fixed antenna (not shown in Fig. 1) on one end of the channel and a MECA 500¹ robot arm that positions a second movable antenna to form a synthetic-aperture array at the other end of the channel in the test volume.

An OptiTrack camera system determines the location, orientation and polarization of the movable antenna as it is scanned. Multiple synthetic-aperture measurements performed by the LSNA over an array of antenna positions characterize the bidirectional relationships between electromagnetic fields generated or received in the test volume and signals received or radiated by the fixed antenna. After replacing the robot with a wireless device under test (DUT), the expected and measured response of the DUT when transmitting or receiving can be compared.

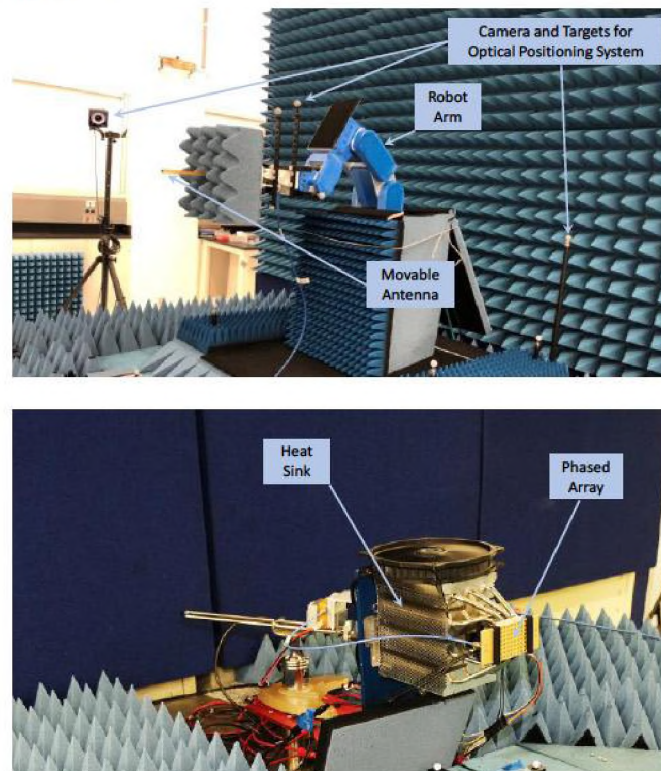


Fig. 1. Photographs of the NIST OTA-Test Environment. Top: Channel characterization with the movable SAMURAI antenna and the Meca 500 Robot Arm. Bottom: Test of a phased array placed in the test volume after removal of the robot arm. Photo taken before new absorber in top photo was added to system.

¹ We use brand names only to specify the experimental conditions and setup. NIST does not endorse commercial products. Other products may work as well or better.

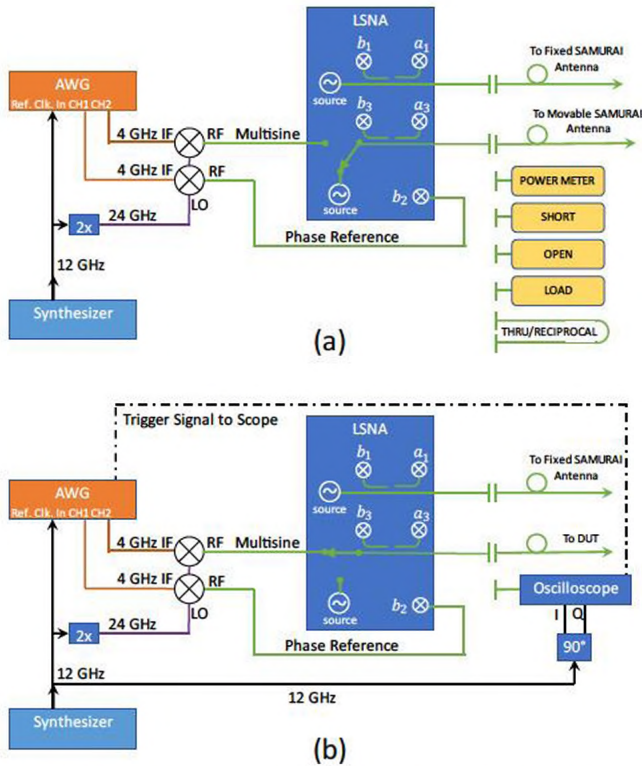


Fig. 2. LSNA measurement system configured to drive DUT, fixed and movable antenna (see Fig. 1, fixed antenna not shown for clarity). (a) Internal sources in the LSNA are used for the scattering-parameter and power calibrations and characterizing channels. Internal LSNA sources are terminated when not generating signals. (b) Signals upconverted from the AWG drive the LSNA during the cross-frequency phase calibration and ensuing modulated-signal predistortion and DUT characterization. A 201-tone AWG-generated Schroeder multisine on a 1 MHz grid was used as a phase reference.

III. INSTRUMENTATION OVERVIEW

Fig. 2 shows a diagram of the LSNA measurement system we used to generate and characterize modulated signals in the SAMURAI system. The two internal sources in the VNA (see Fig. 2(a)) are used to measure the scattering parameters at the WR-28 rectangular-waveguide ports of the two antennas during the characterization of the OTA environment.

A. Modulated-Signal Measurement

We first developed this instrumentation setup for use at lower frequencies [1] and then added upconverters similar to those used in [6] and later in [5] to reach mmWave frequencies, as shown in Fig. 2. This setup allows for the characterization of mmWave modulated signals as implemented in [5, 6] with the added ability to measure on an arbitrary frequency grid, as demonstrated in [1].

As in [1, 5, 6], the synthesizer in Fig. 2 creates a reference tone (12 GHz in these experiments) for the modulated-signal generation and measurement equipment. The reference tone is

used to lock the clock of the arbitrary waveform generator (AWG) to the synthesizer and to synchronize measurements of an equivalent-time sampling oscilloscope to the rest of the system, while a frequency-doubled version of the reference tone is used as the LO for the upconverters.

The AWG creates IF signals centered at 4 GHz that are upconverted to mmWave frequencies by the dual upconverters. The dual upconverters create several signals: a 28 GHz modulated signal that is passed through and characterized by the LSNA before being used to drive the DUT or fixed antenna, a constant phase-reference multisine for the LSNA and two 12 GHz reference sinusoids for correcting the time-base distortion in the oscilloscope [7] and a trigger signal for the oscilloscope.

B. LSNA Calibration

The large-signal scattering-parameter, power and cross-frequency phase calibrations were performed at ports 1 and 3 of the LSNA, which has precision 2.4 mm connectors. After an initial 2.4 mm short-open-load-reciprocal calibration at ports 1 and 3 of the LSNA, the power meter is connected to port 3 and the power from the internal source of the LSNA delivered to that port is measured by both the LSNA receivers and the power meter, as shown in Fig. 2(a). Finally, the 2.4 mm reference calibration was used to set the power and phase calibrations at the WR-28 adapter planes at the DUT input and fixed antenna.

Fig. 2(b) illustrates the cross-frequency phase calibration. First, the equivalent-time sampling oscilloscope, which is calibrated with a photodiode characterized on the NIST Electro-Optic Sampling System [8], is connected to port 3 of the LSNA. Then, the AWG generates a sinusoid at port 3 of the LSNA at each frequency of interest, which is then measured by both the LSNA and the oscilloscope, which captures a 20 ns waveform, enough to fit at least 500 cycles at 28 GHz. The phase measured by the LSNA can then be compared to the phase measured by the traceable oscilloscope with respect to a constant fixed time in each repetition set by the trigger signal and in-phase and quadrature time-base distortion signals, which are measured simultaneously by the oscilloscope [7].

During modulated-signal measurements, the LSNA compares the phase of each of the tones in the modulated signal being characterized to the phase of the corresponding tone in the phase-reference multisine at that same frequency. A calibration on an external computer then determines the phase of the tone in the modulated signal measured by the LSNA. This calibration and measurement procedure not only takes advantage of the existing traceability path from the NIST Electro-Optic Sampling System, but also avoids the fine-frequency-spacing limitations of commercial comb generators and avoids the limitations of the oscilloscope time base on the length of the modulated signals that they can measure.

During the device-characterization stage of the SAMURAI OTA tests, the LSNA can be recalibrated for scattering-parameter and modulated-signal measurements at the DUT input, the DUT output and/or the fixed antenna, and can be driven at any of those ports to allow the DUT to be tested in

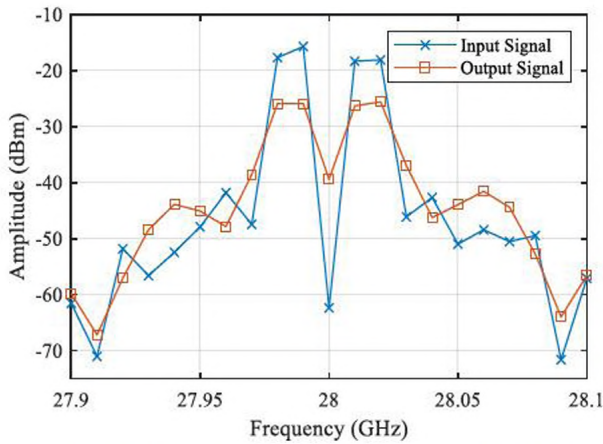


Fig. 3. Spectra of the array input and output 5-tone multisines measured by our system in the NIST OTA test environment.

both transmit and receive modes, or even while simultaneously transmitting and receiving time-domain or frequency-domain multiplexed signals.

IV. MEASUREMENT RESULTS

In the examples shown here, we translated the port 3 calibration to the DUT input and the port 1 calibration to the fixed antenna. In this configuration, the LSNA can measure the modulated signals carried by the forward or backward waves at both the input of the DUT and output of the fixed antenna monitoring the DUT's coaxial and radiated performance.

We demonstrated the system with a 28 GHz programmable phased array designed at Technische Universiteit Eindhoven for research purposes [9]. Then, we configured the LSNA to measure both the pre-distorted modulated signal at the array's coaxial input and the modulated signal transmitted by the array to the fixed antenna through the characterized channel.

A. 10 MHz Multisines

We tested the array with a 5-tone multisine, which we pre-distorted with the LSNA to minimize the center tone at 28 GHz, leaving 4 tones of roughly equal-magnitude with a notch in-between. We did not attempt to pre-distort the out-of-band intermodulation products.

Fig. 3 compares the spectrum of the signal input to the array to the signal radiated by the array as the array was driven into compression. The noise-power ratio (NPR) [10] of the center tone at 28 GHz input into the array was -47 dB, while the NPR of the signal radiated by the array was -12 dB, demonstrating our ability to measure the intermodulation products added to the radiated signal by the array.

We also tested a 9-tone equal-amplitude multisine. Fig. 4 shows the measured phase and amplitude differences at 27.99 and 28.01 GHz between the array's input and output signals as a function of frequency and the array's steering angle. The phases in Fig. 4 are relative to the phase at 28 GHz. (As expected, phase differences and their uncertainty increase near

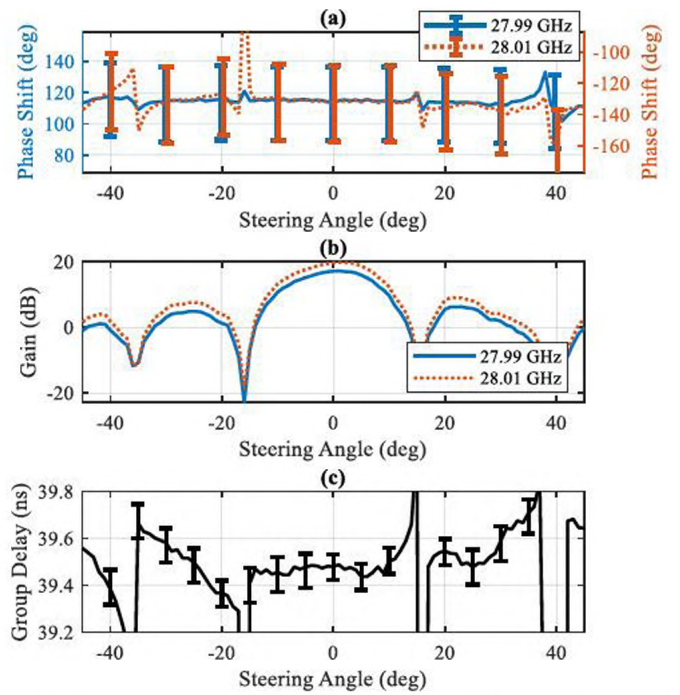


Fig. 4. Phase (a) and amplitude (b) differences of the array input and output tones in the NIST OTA test environment, as well as group delay (c) for multisine waveforms through the measurement system. Phase and delay values are plotted with 95 % confidence intervals.

nulls in the magnitude.)

Because our system includes a cross-frequency phase calibration, we are able to measure both frequency-domain and temporal quantities. Fig. 4(c) illustrates this by plotting the group delay calculated with the phase-detrending algorithm [11] for the 9-tone multisine from the frequency-domain measurements. Note that the peaks in the plotted group-delay occur at array nulls.

B. Uncertainty Evaluation

We evaluated measurement uncertainty with the MUF [3]. The average 95 % confidence intervals we evaluated for the amplitude measurements in Fig. 3 and Fig. 4 were roughly ± 0.19 dB. This uncertainty in power was based on an uncertainty model provided by the manufacturer of the power sensor [12] and our signal-measurement repeatability. A full evaluation is in process and will require establishing traceability directly to the NIST power services.

The uncertainty in the phase difference shown in Fig. 4 is directly traceable to the NIST Electro-Optic Sampling System through the oscilloscope [8]. For steering angles less than ± 15 degrees the phase distortion, as indicated by the difference between the two phase-shift values, is well below our uncertainties.

C. QAM-Like Signal on a 1 MHz Grid

To demonstrate the ability of the system to measure longer calibrated modulated signals, we pre-distorted and measured a

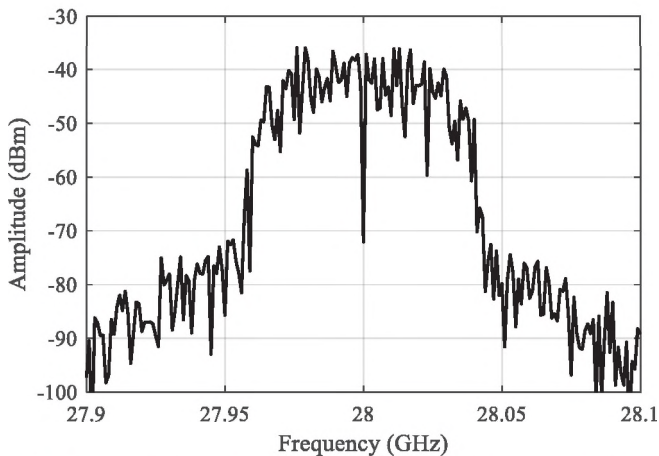


Fig. 5. Predistorted spectrum of a QAM-like multisine measured on a 1 MHz grid in the SAMURAI OTA test environment.

multisine with a spectrum of a typical 80 MHz-wide QAM-like signal on a 1 MHz grid in Fig. 5. A 1 MHz grid is near the limit of what can be achieved with conventional comb generators at 28 GHz. Even on this 1 MHz grid, the signal levels of the tones we used during the calibration and measurements had a signal to noise ratio of about 50 dB.

V. CONCLUSION

We presented a traceable single-instrument approach to OTA test at mmWave frequencies. The LSNA can perform all the network-analysis measurements required for OTA test, including the scattering parameters required to characterize channels in the OTA test environment and the traceable measurement and predistortion of repetitive wideband mmWave modulated signals on arbitrary frequency grids, including the RF, LO and IF frequencies employed and their harmonics and intermodulation products. This approach enables the calculation of temporal quantities such as group-delay from frequency-domain measurement results, while preserving cross-frequency phase. Furthermore, the system is able to monitor all forward and backward channels in the system simultaneously, mismatch-correct all the results and provide uncertainties and their correlations with the MUF [3].

Recently we reduced tone spacings in connectorized measurements of this type to 1 kHz or lower at 28 GHz. Thus, we believe that we should soon be able to achieve these spacings in OTA test systems as well, enabling the measurement of the EVM of millisecond-long repetitive signals with this approach.

ACKNOWLEDGEMENT

We thank A.J. van den Biggelaar and Bart Smolders at the Technische Universiteit Eindhoven for use of the array.

REFERENCES

- [1] A. Sanders, D. Williams, J. M. Kast, K. Remley, and R. D. Horansky, "Large-Signal-Network-Analyzer Phase Calibration on an Arbitrary Grid," presented at the IEEE Int. Microw. Symp., Boston, MA, June 2-7, 2019.
- [2] M. Jordão, R. Caldeirinha, A. S. R. Oliveira, and N. B. Carvalho, "A Survey on Over-The-Air Linearization Methods for MIMO Systems," *Energies*, vol. 14, no. 8, 2021, doi: 10.3390/en14082225.
- [3] *NIST Microwave Uncertainty Framework*. (2011). National Institute of Standards and Technology, <http://www.nist.gov/ctl/rf-technology/related-software.cfm>. [Online]. Available: <http://www.nist.gov/ctl/rf-technology/related-software.cfm>
- [4] A. Weiss *et al.*, "Large-Signal Network Analysis for Over-the-Air Test of Up-Converting and Down-Converting Phased Arrays," in *IEEE Int. Microw. Symp.*, Boston, MA, June 2-7 2019.
- [5] Y. Zhang *et al.*, "Precisely Synchronized NVNA Setup for Digitally Modulated Signal Generation and Measurement at 5G-Oriented Millimeter-Wave Test Bands," *IEEE Transactions on Microwave Theory and Techniques*, vol. 69, no. 1, pp. 833-845, 2021, doi: 10.1109/TMTT.2020.3028383.
- [6] K. A. Remley, D. F. Williams, P. D. Hale, C. M. Wang, J. Jargon, and Y. Park, "Millimeter-Wave Modulated-Signal and Error-Vector-Magnitude Measurement With Uncertainty," *IEEE Trans. Microw. Theory Techn.*, vol. 63, no. 5, pp. 1710-1720, 2015, doi: 10.1109/TMTT.2015.2416180.
- [7] P. D. Hale, C. M. Wang, D. F. Williams, K. A. Remley, and J. Wepman, "Compensation of random and systematic timing errors in sampling oscilloscopes," *IEEE Trans. Instrum. Meas.*, vol. 55, no. 6, pp. 2146-2154, 12/2006 2006.
- [8] T. S. Clement, P. D. Hale, D. F. Williams, C. M. Wang, A. Dienstfrey, and D. A. Keenan, "Calibration of Sampling Oscilloscopes with High-Speed Photodiodes," *IEEE Trans. Microw. Theory Techn.*, vol. 54, no. 8, pp. 3173-3181, 8/2006 2006.
- [9] A. van den Biggelaar, "Over-the-air characterization of millimeter-wave integrated antenna systems," Eindhoven : Technische Universiteit Eindhoven, 2020. [Online]. Available: <https://research.tue.nl/en/publications/over-the-air-characterization-of-millimeter-wave-integrated-anten>
- [10] I. J. Bahl, *Fundamentals of RF and Microwave Amplifiers*. Hoboken, NJ: Wiley, 2006.
- [11] K. Remley, D. Williams, D. Schreurs, G. Loglio, and A. Cidronali, "Phase detrending for measured multisine signals," presented at the ARFTG Microwave Measurement Conference, 2003.
- [12] "Fundamentals of RF and Microwave Power Measurements (Part 3) - Power Measurement Uncertainty per International Guides," in "Fundamentals of RF and Microwave Power Measurements (AN 1449) - Application Note," Keysight Technologies, 2014. [Online]. Available: <https://www.keysight.com/us/en/lib/resources/training-materials/fundamentals-of-rf-and-microwave-power-measurements-an1449-application-note-272209.html>